The paper was presented at the Tenth Meeting
"New Trends in Fatigue and Fracture" (NT2F10)
Metz, France, 30 August–1 September, 2010

Mustapha Allouti, Christian Schmitt, Guy Pluvinage, Michel Lebienvenu

EVALUATION OF THE NOCIVITY OF DENT AND COMBINATION OF DENT AND GOUGE ON BURST PRESSURE OF STEEL PIPE

PROCENA OŠTEĆENJA ULEGNUĆA I KOMBINACIJA ULEGNUĆA I IZDUBLJENJA NA PRITISAK RAZARANJA ČELIČNE CEVI

Original scientific paper
UDC: 620.1:621.643.2 620.1:669.14-462
Paper received: 31.01.2011

Author's address:
LABPS (EA 4632), Ecole Nationale d'Ingénieurs de Metz, Metz, France

Keywords
- nocivity
- dent
- burst pressure
- steel pipe

Ključne reči
- oštećenje
- ulegnuće
- pritisak razaranja
- čelična cev

Abstract

Mechanical damage is the major cause of service failures in Europe in transmission pipelines. A combination of dent and gouge is generally accepted as the most dangerous defect. The main objective of this study is to examine the influence of this kind of defect on burst pressure of A37 steel pipes. Experimental burst tests are carried out on pressure vessels. The gouge which is obtained with Electrical Discharge Machining has the same geometry for all specimens. The tests show that failure occurs on other place than that of the defect, except for the smallest dent depth. The stress distribution at the gouge tip is obtained with finite element simulation. A criterion based on stress triaxiality and effective stress is proposed in order to explain the burst test results.

Izvod

Mehaničko oštećenje je glavni uzrok otkaza sistema kod transportnih cevovoda u Evropi. Kombinacija ulegnuća i izdubljenja se uopšteno smatra za najopasniji oblik greške. Glavni cilj ovog rada je proučavanje uticaja ovog tipa greške na pritisak razaranja cevi od A37 čelika. Eksperimentalna ispitivanja razaranjem pod pritiskom se izvode na posudama pod pritiskom. Izdubljenje, izvedeno elektroerozijom, je potpuno iste geometrije kod svih epruveta. Ispitivanja pokazuju da se lom javlja na drugom mestu u odnosu na mesto greške, osim kod udubljenja najmanje dubine. Raspodela napona na vrhu izdubljenja dobijena je simulacijom konačnim elementima. Predložen je kriterijum na osnovu troosnosti napona i efektivnog napona radi objašnjenja rezultata razaranja pritiskom.

INTRODUCTION

Several types of defects can be found in gas or oil transmission pipelines: internal or external corrosion craters, material defects, weld cracks due to improper welding, fatigue cracks, and mechanical damages due to external interferences. A recent study has shown that about the half of failures of transmission pipes is due to mechanical damages [1]. These damages can be classified into dents and gouges.

A dent causes a local reduction in the pipe diameter and is considered as a non severe defect. In literature, one can find some empirical rules which define critical dent depths /2, 3, 4, 5/.

A gouge in a pipe is characterised by material removing on pipe surface. The removed volume is characterised by a high length to width ratio and a sharp notch profile: The gouge is inclined from an angle to the pipe longitudinal direction. Limit analysis and notch fracture mechanics can be used in order to assess gouge nocivity. Limit load given by limit analysis is based on the following criterion: failure occurs by plastic collapse when effective net stress reaches the local ultimate strength of the material. For pipes subjected to internal pressure, codes and methods used in literature give different definitions of hoop stress and local ultimate strength /6, 7, 8/.

A combination of dent and gouge is generally accepted as the most dangerous defect and its behaviour is not well understood. Dent + gouge defect combines a severe defect (the gouge) with a non severe one (the dent): a simple approach consists to correct the gouge solution in order to take into account the presence of the dent. The Batelle Institute has carried out burst tests and proposed an empirical relationship between the failure stress and the Charpy energy through a parameter called Q parameter which is a function of Charpy energy of material and the geometry of the gouge and dent /9/. The Batelle formula is limited to $Q > 16.33$ m·kg·cm^{-1} (300 ft·lbf·in^{-1}) and cannot

be used for many failure cases. British Gaz has proposed a very complex formula to determine the circumferential fracture stress of a pipe with a combined gouge + dent defect and based on a collapse modified strip-yield model /10/. It includes expressions for the stress state at the base of the dent, and considers the interaction between fracture and plasticity.

In this work, dent and combined dent + gouge defects are studied. Experimental burst tests are carried out on pressure vessels in order to evaluate the influence of the geometry of the defect on the critical burst pressure. The finite element method is applied to investigate the stress distribution around the defect. For dent, Oyane's criterion is used and for combined defect, a criterion based on notch fracture mechanics and stress triaxiality is proposed.

EXPERIMENTAL STUDY

Material and specimens

Pressure vessels are made of A37 pipe steel. Mechanical properties and chemical composition of this steel are given in Tables 1 and 2.

Table 1. Mechanical properties of A37 steel.
Tabela 1. Mehaničke osobine čelika A37

Young's modulus E (MPa)	Poisson's ratio ν	Yield stress σ_y (MPa)	Ultimate strength σ_u (MPa)	Elongation A (%)
202 500	0.3	355	431	30

Table 2. Chemical composition of A37 steel.
Tabela 2. Hemijski sastav čelika A37

C	Si	Mn	P	S	Cr	Ni	Mo	Al	Cu
0.085	0.22	0.5	0.01	0.0025	0.84	0.115	0.046	0.026	0.165

In order to limit the stiffening effect of the end caps, the pipe length is equal to 6.74 times the outer diameter. Pressure vessels have been made with pipe pieces of length L = 600 mm, thickness t = 3.2 mm and external diameter D_e = 88.9 mm (see Fig. 1). Pipe ends are covered with caps described in Fig. 2. A valve is welded on one cap in order to apply an internal water pressure.

Dents are obtained by applying a rigid spherical indenter tooth (40 mm in diameter) at low strain rate with a tension testing machine. For dent alone, five dent depth are studied, dent depth being defined as the maximum reduction in the diameter of the pipe compared to the original diameter. Their geometry is given in Table 3.

For combined defect, three dent depths are studied. A gouge is made by electro spark discharge at the bottom of the dent after indentation. The geometry of the gouge is the same for all the specimens tested: length: 6.4 mm, depth: 1.6 mm, width: 2 mm, and notch radius: 1 mm. For all specimens, the gouge direction is parallel to the longitudinal axis of the vessel. Figure 3 shows the geometry of the combined defect. The geometry of the combined defect is given in Fig. 3 and in Table 4.

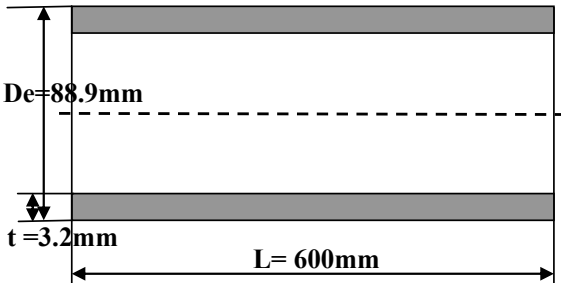

Figure 1. Pipe geometry.
Slika 1. Geometrija cevi

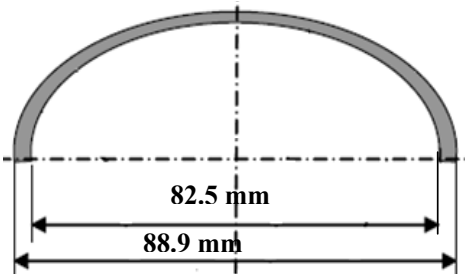

Figure 2. Cap geometry.
Slika 2. Geometrija danca

Table 3. Dent geometries and experimental burst pressures (dent alone).
Tabela 3. Geometrije ulegnuća i eksperimentalni pritisci razaranja (samo za ulegnuće)

Vessel number	1	2	3	4	5
Dent depth (mm)	≈ 25 (≈ 28% D_e)	≈ 14 (≈ 16% D_e)	≈ 11.8 (≈ 13% D_e)	≈ 8.9 (≈ 10% D_e)	≈ 8.9 (≈ 10% D_e)
Burst pressure (MPa)	31.3	31.0	31.6	30.8	31.0
Dent width 2c (mm)	–	50	44	40	–

Table 4. Dent geometry and experimental burst pressures.
Tabela 4. Geometrija ulegnuća i eksperimentalni pritisci razaranja

Vessel number	1	2	3
Dent depth (mm)	≈ 16% D_e	≈ 10% D_e	≈ 4% D_e
Burst pressure (bar)	309	308	302
Failure location	smooth wall	smooth wall	gouge

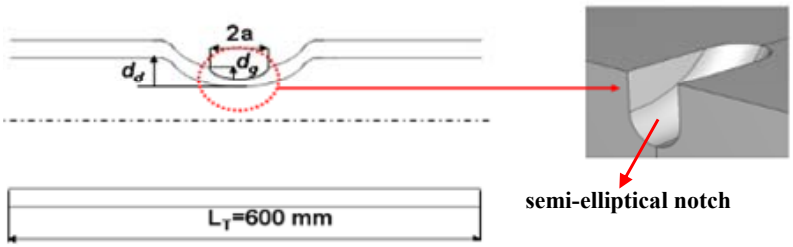

Figure 3. Geometry of combined gouge + dent defect introduced longitudinally in a pressure vessel.
Slika 3. Geometrija kombinovanog izdubljenja + ulegnuća uvedenih podužno na posudu pod pritiskom

Burst tests results

For dent alone, critical (burst) pressures for the 5 tests are given in Table 3. It is to be noted that there is no effect on dent geometry on burst pressure. Critical pressure P_L is close to limit pressure given by the simple formula (P_L = 31 MPa):

$$P_L = \frac{\sigma_u t}{R} \quad (1)$$

Where σ_u is the ultimate strength (σ_u = 431 MPa, determined by uniaxial tension test), t is the wall thickness (t = 3.2 mm) and R is the outer radius of pipe (R = 44.45 mm).

We note that the burst pressure of vessel without defect (dent) is equal to 31.1 MPa. It can be noted that failure occurs on other places than that of the dent as we can see on Fig. 4a, b, c and d.

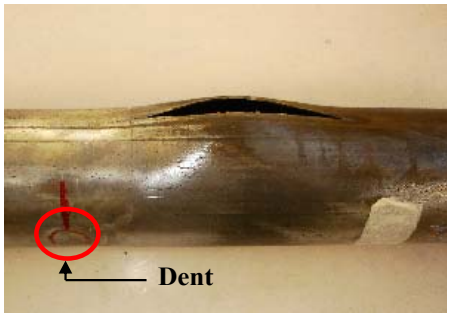

(a) Vessel 1: Dent depth ≈ 25 mm (≈ 28% D_e); Burst pres. = 31.3 MPa

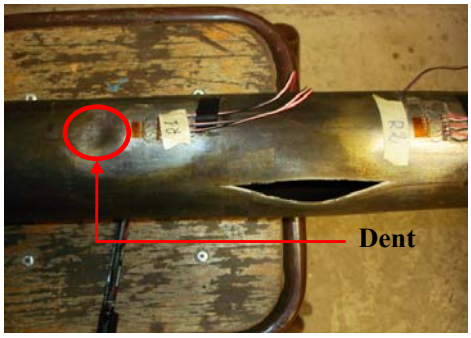

(b) Vessel 2: Dent depth ≈ 14 mm (≈ 16% D_e); Burst pres. = 31.0 MPa

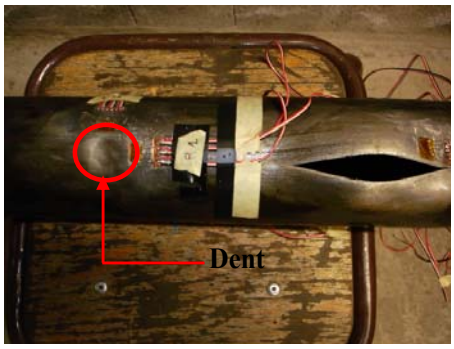

(c) Vessel 3: Dent depth ≈ 11.8 mm (≈ 13% D_e); Burst pres. = 31.6 MPa

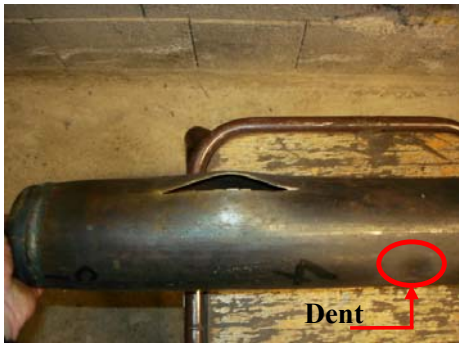

(d) Vessel 4: Dent depth ≈ 8.9 mm (≈ 10% D_e); Burst pres. = 30.8 MPa

Figure 4. Location of tearing opening after burst tests of the indented vessels.
Slika 4. Mesta otvaranja cepanjem nakon ispitivanja razaranjem posuda sa ulegnućem

For combined dent + gouge defect, critical (burst) pressures for the three tests are given in Table 4. It can be noted that:

– The failure occurs at gouge tip only for a dent depth of 4% of the external diameter (Fig. 5). For greater dent depth, localisation of vessel failure is outside of the defect in a smooth part of the specimen.
– The burst pressure is close to those of a vessel without defect (31.1 MPa).

Figure 5. Combined defect of ves. 1 (dent depth ≈ 4%D_e) after failure.
Slika 5. Kombinovana greška pos. 1 (dub. uleg. ≈ 4%D_e) posle loma

NOTCH FRACTURE MECHANICS FOR COMBINED DENT + GOUGE NOCIVITY ASSESSMENT: VOLUMETRIC METHOD

The Volumetric Method /11/ is a local fracture criterion which assumes that the fracture process requires a certain volume. This volume is assumed as a cylindrical volume with effective distance as its diameter. Physical meaning of this fracture process volume is "the high stressed region" where the necessary fracture energy release rate is stored. The difficulty is to find the limit of this "high stressed region". This limit is *a priori* not a material constant but depends on loading mode, structure geometry and load level. The size of the fracture process reduced to the effective distance X_{ef} according to the above mentioned assumptions is obtained by examination of the stress distribution.

The bi-logarithmic elastic-plastic stress distribution (Fig. 6) along the ligament exhibits three zones which can be easily distinguished. The elastic-plastic stress primarily increases and it attains a peak value (zone I) then it gradually drops to the elastic plastic regime (zone II). Zone III represents linear behaviour in the bi-logarithmic diagram. It is proved by examination of fracture initiation sites that the effective distance corresponds to the beginning of zone III which is in fact an inflexion point on this bi-logarithmic stress distribution. A graphical method based on the relative stress gradient χ associates the effective distance to the minimum of χ. The relative stress gradient is given by:

$$\chi(r)=\frac{1}{\sigma_{yy}(r)}\frac{\partial\sigma_{yy}(r)}{\partial r} \tag{2}$$

where $\chi(r)$ and $\sigma_{yy}(r)$ are the relative stress gradient and maximum principal stress or opening stress, respectively.

The effective stress for fracture is then considered as the average value of the stress distribution over the effective distance:

$$\sigma_{ef}=\frac{1}{X_{ef}}\int_0^{X_{ef}}\sigma_{yy}(r)dr \tag{3}$$

Therefore, the notch stress intensity factor is defined as a function of effective distance and effective stress:

$$K_\rho=\sigma_{ef}(2\pi X_{ef})^\alpha \tag{4}$$

where K_ρ, σ_{ef} and X_{ef} are notch stress intensity factor, effective stress and effective distance, respectively, α is the slope of the stress distribution in region III.

Description of this kind of stress distribution at notch tip and the relative stress gradient are given in Fig. 6.

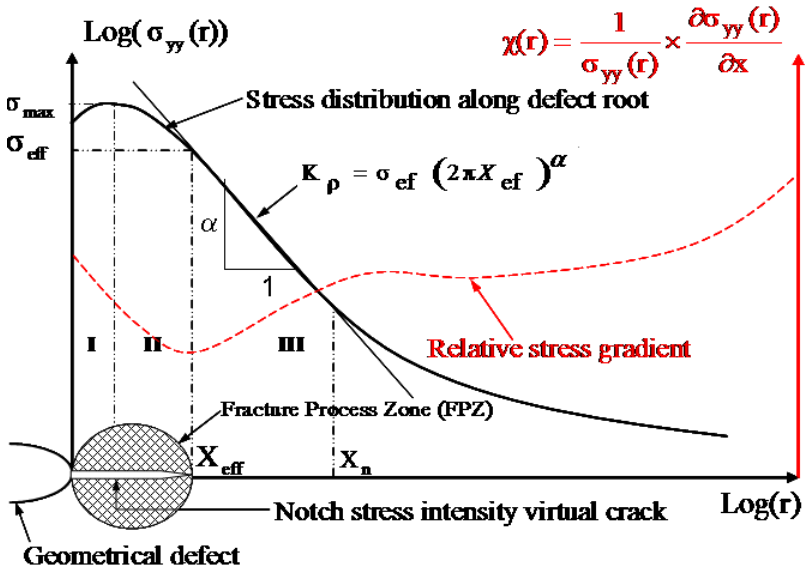

Figure 6. Schematic elastic-plastic stress distribution along notch ligament and notch stress intensity virtual crack concept.
Slika 6. Shema koncepcije raspodele elastoplastičnog napona duž ligamenta zareza i intenzitet napona zareza virtualne prsline

NUMERICAL SIMULATION

A finite element simulation using ABAQUS software is realised. Vessel models are designed using 8-nodes hexahedral elements. Elastic-plastic behaviour is modelled using an isotropic strain hardening law. Cap effect is simulated by applying a pressure on the other end of the pipe. Symmetry conditions permit modelling of only one-quarter of the specimen with appropriate constraints imposed on the symmetry plans.

Three steps analysis is used in order to reproduce experimental conditions:

- First step: the vessel is dented with a rigid spherical indenter.
- Second step: the indenter is removed. One can note a spring-back phenomenon.
- Third step: pressurization of the vessel. The dent moves outwards allowing the pipe to regain partially its circular shape.

Figure 7 gives an example of mesh in the vicinity of a gouge.

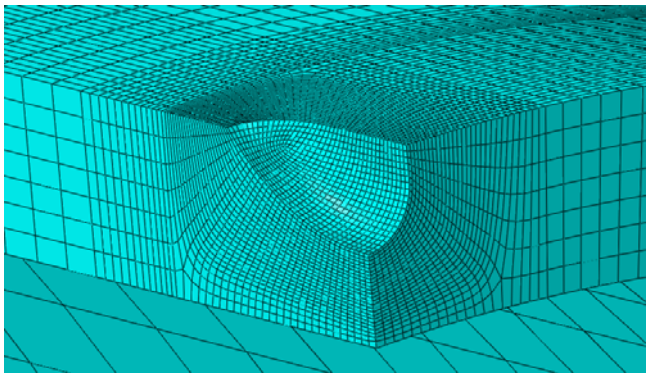

Figure 7. Example of mesh used for the finite element simulation.
Slika 7. Primer mreže za simulaciju konačnim elementima

RESULTS AND DISCUSSION

Oyane's criterion for the dent defect

We propose a novel approach to predict damage and failure of pressurized pipe with dent. This approach is based on simple local strain criterion and considers also the dent as any indentation. Based on various assumptions, many criteria for ductile fracture due to deep drawing have been proposed /12, 13, 14, 15/. In the present study, we use the criterion proposed by Oyane et al. /12/:

$$\left.\begin{aligned} I=\int_0^{\bar{\varepsilon}_f}\left(C_1+\frac{\sigma_m}{\bar{\sigma}}\right)d\bar{\varepsilon}=C_2 \\ I=\frac{1}{C_2}\int_0^{\bar{\varepsilon}_f}\left(C_1+\frac{\sigma_m}{\bar{\sigma}}\right)d\bar{\varepsilon}=1 \end{aligned}\right\} \quad (5)$$

where $\bar{\varepsilon}_f$ is the equivalent strain at which the fracture occurs, σ_m is the hydrostatic stress, $\bar{\sigma}$ is the equivalent stress, $\bar{\varepsilon}$ is the equivalent strain, and C_1 and C_2 are the material constants. To determine the material constants C_1 and C_2 in Eq. (5), tests have to be performed under two types of stress conditions: uniaxial and plane-strain tension tests.

By finite element simulation, I integral is calculated for each element and each deformation step /16/.

From Eq. (5), it can be assumed that the fracture criterion is satisfied in a given element, provided that the I integral reaches the value of one, so fracture occurs.

Oyane's criterion values are given as a function of step times during the three steps of calculation. Figure 8 gives evolution of I values for different dent depth during the application of indentation and pressurization.

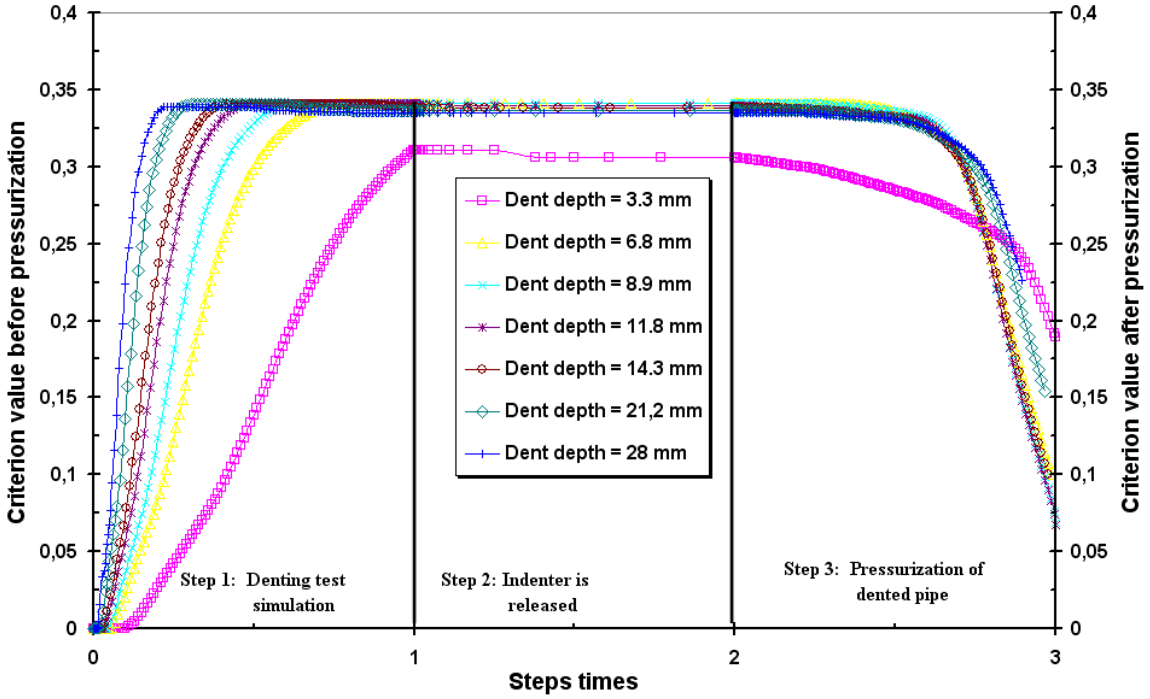

Figure 8. Evolution of the maximum Oyane criterion value during three steps of calculation ($C_1 = -0.172$ and $C_2 = 0.3$).
Slika 8. Razvoj maksimalne vrednosti Ojan kriterijuma tokom tri koraka proračuna ($C_1 = -0.172$ i $C_2 = 0.3$)

We notice that all curves have the same behaviour characterised by three phases, indicated as phase I, II and III.

Phase I. There is a linear increase in the value of failure criterion for all dent depths.

Phase II. Stabilization.

Phase III. The criterion value decreases under the influence of internal pressure pipe because the latter tends to push out the dent, thus reducing the dent depth.

To better understand why vessel failures do not occur at dent location but elsewhere, we have measured Vickers micro hardness at the base and away from the dent. Statistical analysis is given in Table 5. We note that the Vickers micro hardness values measured at the base of dent are higher than those measured outside.

Table 5. Statistical analysis of HV micro hardness results
Tabela 5. Statistička analiza rezultata HV mikrotvrdoće

	Mean Vickers micro hardness	Standard deviation	σ_u (MPa)	P_L (MPa)
Away from dent	136	5.4	431	31.0
At base of dent	177	15.2	561	40.4

One can notice that there is approximately 30% difference between the two mean values. These Vickers micro hardness values are converted into ultimate strength by using the conversion table /17/ and reported in Table 5. Limit pressure values (P_L) are calculated according to Eq. (1) and reported in Table 5. We note a difference of about 30%, which is enough to explain that fracture cannot occur at dent because of the increase of ultimate strength due to stain hardening.

Stress distribution and failure criterion for the combined dent + gouge defect

Finite element computation provides stress distribution ahead of the gouge tip. Using the procedure described in the earlier section, we obtain the effective stress and use it for a failure criterion.

In order to compare the stress distribution of a combined dent + gouge defect to those of a gouge alone, we have tested a "reference" vessel containing a "critical" gouge taken as reference. The geometry of this critical gouge is: length 32 mm, depth 2.4 mm (3*t*/4), and notch radius 0.5 mm.

Example of typical stress distribution at gouge tip can be seen in Fig. 9 for the gouge alone (reference) and for the defect gouge + dent. One note that the stress distribution is similar with an important change in slope in zone III of the stress distribution. The similarity between the stress distribution supports the assumption that the combined defect gouge + dent can be treated by the same solution of a gouge i.e. *Volumetric Method*. The important change of the slope in region III is due to the bending moment induced by the movement of dent walls with pressure.

One notes that the effective stress decreases with dent depth. The additional bending stress distributions modify the final distribution and reduce its severity and consequently the stress triaxiality β.

$$\beta = \frac{\sigma_m}{\sigma_{eq}} \tag{6}$$

where σ_m is the hydrostatic stress and σ_{eq} the Von Mises equivalent stress.

Due to the fact that the failure of the pipe is ductile and taking into account the fact that ductile failure is sensitive to stress triaxiality, its average value is computed using this formula:

$$\bar{\beta}_c = \frac{1}{X_{ef}} \int_0^{X_{ef}} \beta_c(r)dr \tag{7}$$

We note in Table 6 that the stress triaxiality decreases with the dent depth which then decreases the severity of a gouge + dent defect. In this table, dent depth "0%D_e" corresponds to the "critical" gouge alone taken as reference.

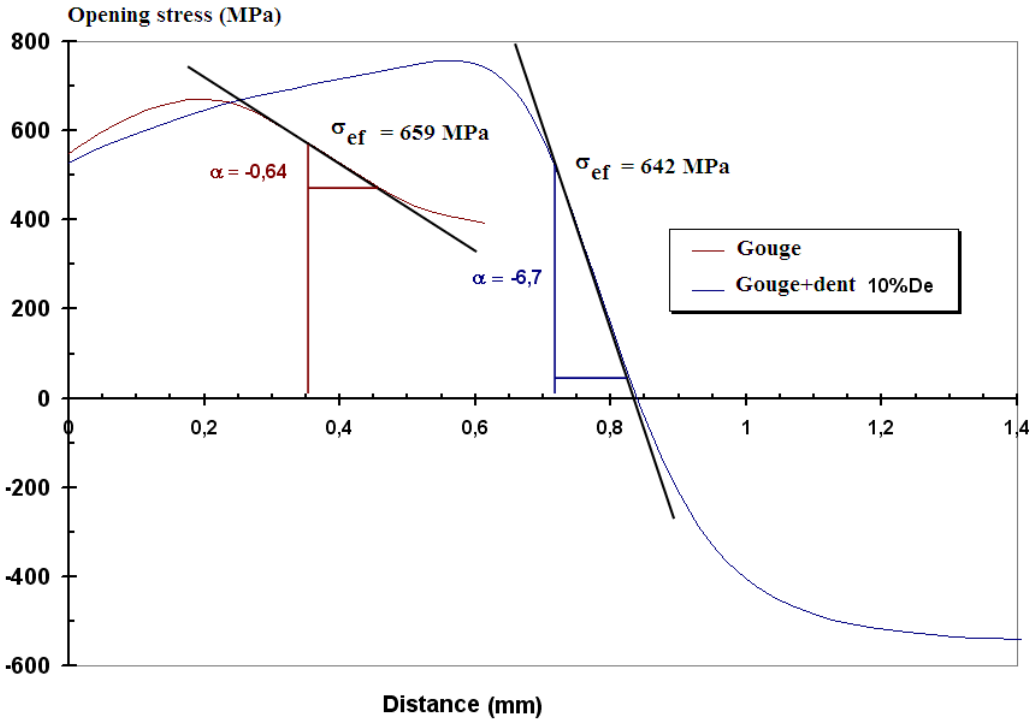

Figure 9. Stress distribution ahead of defect tip (gouge and gouge + dent).
Slika 9. Raspodela napona ispred vrha greške (izdubljenje i izdubljenje + ulegnuće)

Table 6. Results of effective stress and stress triaxiality for combined gouge and dent defect.
Tabela 6. Rezultati efektivnog napona i troosnosti napona za kombinovanu grešku izdubljenja i ulegnuća

Dent depth	0% D_e	4% D_e	10% D_e	16% D_e
Effective stress (MPa)	642	677	659	637
Effective distance (mm)	0.37	0.81	0.72	0.66
Slope α	–0.64	–6.38	–6.7	–6.9
Average critical stress triaxiality $\overline{\beta}$	0.79	0.85	0.8	0.75
σ_{ef} $\overline{\beta}$ (MPa)	507	575	527	477
Failure location	gouge	gouge	smooth wall	smooth wall

The influence of the bending stress distribution due to dent is obtained by comparing the product of the critical effective stress and critical average stress triaxiality. Location of failure at gouge is obtained by the following criterion:

$$\sigma_{ef}\overline{\beta} \le \sigma_{ef}^{c}\overline{\beta}_{c} \tag{8}$$

where σ_{ef}^{c} and $\overline{\beta}_{c}$ are the value of critical effective stress and average triaxiality for a single gouge.

This criterion does not work for a dent with a depth 10% of external diameter: this is attributed to uncertainties of material properties.

CONCLUSION

Dents are one of less harmful defect types able to cause fracture of pressurized pipes; it is the less severe defect compared to the other: cracks, corrosion craters, gouges and dents + gouges.

Dent assessment is currently made by using the "10% rule" where a dent having a depth superior to 10% of the pipe diameter is not accepted. According to our results, it seems that this empirical rule is very conservative.

Combined gouge + dent defects cannot be considered as crack-like defect and treated by classical fracture mechanics. In this case the procedure is inappropriate and too much conservative. Combined gouge + dent defects induce elastic-plastic failure and can be assessed by notch fracture mechanics. In this work, we have proposed a simple criterion based on effective stress and stress triaxiality which is in good accordance with experimental burst tests results.

REFERENCES

1. 7th Report of European Gas Pipeline Incident Data Group, 1970-2007, Gas pipeline Incidents, 1-33, 2008.
2. Eiber, R.J., The effect of dents on the failure characteristics of pipeline, Batelle Colombus Laboratories. NG 18, Report N°125, May 1981.
3. Jones, D.G., *The Significance of Mechanical Damage in Pipelines*, 3R International, 21, Jahrgang, Heft, 1982.
4. Fitness-for-Service. API Recommended Practice 579, 1st Ed. American Petroleum Institute; January 2000.
5. Roovers, P., Bood, R., Galli, M., Marewski, U., Steiner, M., Zaréa, M., *EPRG Methods for Assessing the Tolerance and Resistance of Pipelines to External Damage*, Pipeline Technology, Volume II, Proceedings of the Third International Pipeline Technology Conference, Brugge, Belgium, R. Denys, Ed., Elsevier Science, 405-425, 2000.
6. ASME B31G-1991, Manual for determining the remaining strength of corroded pipelines, The American Society of Mechanical Engineers, New York, USA, 1991.
7. DNV-RP-F101, Corroded pipelines, Det Norske veritas, 1999.
8. Choi, J.B., Goo, B.K., Kim, J.C., Kim, Y.J., Kim, W.S., *Development of limit load solutions for corroded gas pipelines*, Int. J. Pressure Vessels Piping, 80, 2, 121-128, 2003.
9. Eiber, R.J., Maxey, W.A., Bert, C.W., McClure, G.M., The Effects of Dents on the Failure Characteristics of Linepipe, Battelle Columbus Laboratories, NG-18, Report No. 125, AGA Catalogue No. L51403, 1981.
10. Hopkins, P., *The application of stiffness for purpose methods to defects detected in offshore transmission pipelines*, Int. Conf. on welding and weld performance in the process industry, London, 1992.
11. Adib, H., Jallouf, S., Schmitt, C., Carmassol, A., Pluvinage, G., *Evaluation of the effect of corrosion defects on the structural integrity of X52 gas pipelines using the SINTAP procedure and notch theory*, Int. J Pressure Vessels Piping, 84, 3, 123-131, 2007.
12. Oyane, M., Sato, T., Okimoto, K., Shima, S., *Criteria for ductile fracture and their application*, J. Mech. Work Technol., 4, 1980.
13. Clift, S.E., Hartley, P., Stugress, C.E., Rowe, G.W., *Fracture prediction in plastic deformation processes*, Int. J Mech. Sci., 32, 1990.
14. Brozzo, P., Deluca, B., Rendina, R., *A new method for the prediction of formability in metal sheets*, Proceedings of 7th Biennial Conference of IDDRG on Sheet Metal Forming and Formability, 1972.
15. Takuda, H., Mori, K., Fujimoto, H., Hatta, N., *Prediction of forming limit in deep drawing of Fe/Al laminated composite sheets using ductile fracture criterion*, J Mat. Proc. Technol., 60, 1996.
16. Takuda, H., Mori, K., Hatta, N., *The application of some criteria for ductile fracture to the prediction of the forming limit sheet metals*, J Mat. Pro. Technol., 95, 1999.
17. ArcelorMital, http://www.arcelormittal.com/fce/repository/transfer/Tablesdeconversion.pdf , April 2005.